



Contents list available at CBIORE journal website

International Journal of Renewable Energy Development

Journal homepage: <https://ijred.cbiorc.id>



Research Article

Consideration of various configurations of SG6043-based rotor applied in small capacity horizontal axis wind turbine

Thin Dinh Van^a, Duc Nguyen Huu^{a*}, Sang Le Quang^b

^aFaculty of Energy Technology, Electric Power University, Vietnam.

^bInstitute of Science and Technology for Energy and Environment, Vietnam Academy of Science and Technology, Vietnam.

Abstract. The SG6043 airfoil model is well known for its high aerodynamic efficiency and it is suitable for designing small wind turbine blades. This paper determined the optimal blade configurations using only the SG6043 airfoil model with ten different lengths from 1 m to 10 m. Then, it proposed the most suitable model for a rated wind speed of 5 m/s in Vietnam. The chord and twist values of each blade's part were optimized by using the Betz optimization method (BOM) in the Qblade open software. Several important characteristic quantities such as lift coefficient (C_l), drag coefficient (C_d), power factor (C_p) and power (P) of the different blade configurations are determined by using a combination of both XFRL5 code and Qblade software. After that, parameters related to operation such as pitch angle and rotation speed of the rotor were also investigated to find the operating conditions for the best efficiency of wind energy exploitation. The obtained results show that the C_p of the blades has a maximum value of about 0.476 and the P has a value of up to 95.319 kW in operating conditions with a wind speed range between 1 m/s and 10 m/s. In addition, the ratios of power to blade surface area (P/S) and the ratios of power to blade volume (P/V) at the wind speed of 5 m/s were also investigated. The results show that rotors with blades ranging from 3 m to 5 m will give much higher P/S and P/V values than other blade configurations under these operating conditions. This emphasizes that these blade configurations will bring more economic benefit because they will consume less material and reduce production time while still ensuring the required capacity value. Finally, the 5 m blade rotor with a capacity of 2.750 kW at a rated wind speed of 5 m/s was proposed as the rotor suitable for individual household use. This design can help millions of Vietnamese households be proactive in their power source, thereby contributing to the significant reduction of CO₂ emissions from coal-fired power plants.

Keywords: SG6043 Airfoil, Low Wind Speed, Small Horizontal Axis Wind Turbines (SHAFT), Betz Optimization Method (BOM), Qblade Software.



@ The author(s). Published by CBIORE. This is an open access article under the CC BY-SA license (<http://creativecommons.org/licenses/by-sa/4.0/>).

Received: 29th Dec 2023; Revised: 16th Feb 2024; Accepted: 13th March 2024; Available online: 21st March 2024

1. Introduction

Currently, wind energy is taking a larger share in the electricity generation sector, which then helps to achieve the target of CO₂ emission. According to the (International Renewable Energy Agency (IRENA) 2022), humanity needs to work to cut 37 Gt of annual CO₂ emissions by 2050. To obtain this goal, countries need to add 248 GW of wind power each year.

Over the long history of wind power, mankind has always sought to build wind farms using giant turbines. The larger the turbine, the higher energy is obtained (U.S. Energy Information Administration (EIA) 2023). The rotor diameter of wind turbines has increased to 140 m by the end of 2022 and could reach 250 m by 2035 (Wind Energy Technologies Office 2023). However, in order to work effectively, these huge turbines should be installed in places with high wind speeds. This leads to the problem that we only focus on exploiting high-velocity wind regions and neglecting low-velocity areas. According to the report of the (Institute of Energy 2023) the technical exploitation potential of onshore wind in Vietnam is 221 GW. However, the potential wind capacity in areas with wind speeds higher than 5.5 m/s is only 57 GW, and the potential wind capacity is 164

GW for areas with low wind speeds from 4.5 m/s to 5.5 m/s. The report of the (Institute of Energy 2023) also pointed out that Vietnam needs to install about 70 GW of onshore wind power capacity by 2050 in a great effort to achieve a net zero emissions scenario. Therefore, it is necessary to fully exploit areas with wind speeds around 5 m/s. As a result, it is essential to study small wind turbines to effectively exploit these low-velocity wind regions.

Turbine blades are made up of different airfoil patterns. Airfoil patterns will be placed at the most appropriate twist angles to obtain the largest ratio between lift and drag force. Several studies introduced designs of airfoil patterns and the optimal arrangement of the airfoil patterns (Manwell *et al.* 2009; Karthikeyan *et al.* 2015; Krishnan *et al.* 2023; Suhas *et al.* 2023). The typical power range of small wind turbines is from 20W to 100kW. Figure 1 illustrates typical sizes of small wind turbine used in residential applications.

In recent years, several researchs introduced methods of designing blades at low wind speeds. In the research (Giguere *et al.* 1998), experimental studies were conducted to compare the maximum ratio between lift coefficient and drag coefficient (C_l/C_d) of the best airfoil models in the Reynolds number range from 100000 to 500000. In this study, Giguere *et al.* compared

* Corresponding author
Email: ducnh@epu.edu.vn (D.N. Huu)

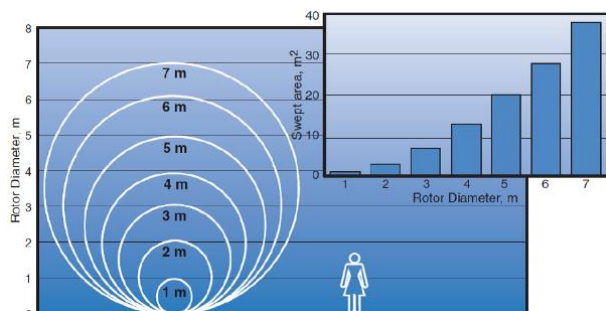


Fig 1. Typical sizes of small wind turbine (WindExchange 2023)

models of the SG604X group with E387 model, Clark-Y model, SD7032 model, FX63-137 model and many others. Finally, the research pointed out that the SG6043 airfoil model has the highest value of the maximum C_l/C_d at Reynolds number of 300000 and concluded that the SG6043 airfoil model is suitable for the blade design of small horizontal axis wind turbines (SHAWTs) with capacities from 1 kW to 5 kW. This result is a good reference for other studies to develop further.

Nowadays, several research groups have also published turbine blade designs using the SG6043 airfoil model with different operating conditions. In the paper of (Umar *et al.* 2022), this team used the blade element momentum (BEM) method for different Reynolds number and tip speed ratio (TSR) parameters with the NACA4412 and SG6043 models. Finally, this research determined that the rotor using a blade length of 1 m and $TSR=4$ is optimal for both the NACA4412 and SG6043 at wind speeds of 4 m/s. The power of these turbines is 79.3 W and 80.1 W at the 4 m/s rated wind speed and the starting wind speed of 1.8 m/s and 1.7 m/s, respectively. The published results of these studies showed the superiority of the SG6043 airfoil model compared to the NACA4412 airfoil model. However, the capacity of these turbines is too small and cannot meet the minimum needs of any household. On the other way, another study (Akbari *et al.* 2022) also conducted comparative analyses of SG6043 airfoil model with many different models using the differential evolution optimization technique to give the best blade design in terms of C_p and startup time of a 1000 W turbine. Finally, the proposed design is the blade using SG6043 airfoil model with a length of 1.21 m, $TSR=5.71$ and a rated wind speed of 10 m/s. Similarly, with a power of around 1000 W, the research of (Daniyan *et al.* 2018) also proposed an optimized blade design based on the SG6043 airfoil model, the blade length is 0.5m with $TSR=6$, this blade has a capacity of 1108 W at a rated wind speed of 18 m/s. However, the values of rated wind speed in these studies are somewhat impractical for the operation of SHAWTs. Because it is obvious to install large wind turbines in such areas with good wind resources.

For a larger power range, the research of (Mwanyika *et al.* 2021) presented a blade design based on the SG6042 and SG6043 models using composite materials. This paper used the BEM method to design the blades and then applied computational fluid dynamics (CFD) to determine the best layout. Consequently, the best blade design based on the SG6043 with a length of 3.56 m, $TSR=6$ was found. This design can generate a nominal power of 5258 W at a rated wind speed of 8 m/s. With equivalent power, the research of (Mostafa *et al.* 2014) introduced a blade design based on the SG6043 airfoil model with 4.455 m length, $TSR=11$ and a capacity of 5128 W at a rated wind speed of 6 m/s and the other configuration with a length of 2.424 m, $TSR=11$ and a nominal power of 5125 W at a rated wind speed of 9 m/s. Those designs are more practical than those of previous publications, because a turbine with a

capacity of about 5 kW operating at a wind speed of about 6 m/s is suitable for most areas in the world. Considering the larger capacity wind turbines, the study of (Shin *et al.* 2019) used a genetic algorithm to optimize the chord and twist values of the blade using SG6043 airfoil model. From that, a design with a blade of 7.25 m in length, $TSR=7.53$, and a nominal power of 32,000 W at a wind speed of 10 m/s was proposed. Designing the turbines with blade lengths longer than 7m will provide greater capacities, however these designs require a larger areas to install.

Obviously, the SG6043 airfoil model is an aerodynamic efficiency model and suitable for designing the blades of SHAWTs that operate at wind speeds of less than 10 m/s. However, in those studies, only one blade configuration with one or several blade lengths were researched. Different blade configurations have been not fully investigated. On the other hand, the SG6043 airfoil model outperformed in comparison with others only in the low Reynolds regions, thus studies focusing on wind velocities greater than 10m/s were not so practical.

This paper aims to carry out research on blade configuration types of a small wind turbine which is suitable for typical low wind speeds in Vietnam, especially with a wind speed of 5 m/s. Key contributions of this study are as: (1) to propose the most suitable model with a wind speed of 5m/w by using the Betz optimization method; (2) to determine the optimal designs in practical use for Vietnam.

The rest of the paper is organized as follows. Section 2 introduces the optimal method for designing turbine blades. The results and discussions are presented in Section 3. Finally, the conclusions are drawn in Section 4.

2. Methodology

Based on the shortcomings of previous publications, this article presents the blade designs based on the SG6043 airfoil model with different lengths from 1 m to 10 m. These analyzing models operate in areas with wind speeds from 1 m/s to 10 m/s. Then, the optimal design of the rotor suitable for a wind speed of 5 m/s was proposed. The BOM method was used to design the turbine blades, after that the rotor parameters were also be determined based on a lifting line free vortex wake method (LLFVWM). These two methods were integrated into the Qblade V.2.0.6.3 Beta and XFLR5 code. In the next stage, the blade configurations were analyzed based on the parameters of surface area and volume. These parameters will directly affect the material cost and fabrication time of the blades using 3D printing technology. In recent years, 3D printing technology has been strongly developed and promised to bring many great benefits in the field of technology production.

2.1 The lifting line free vortex wake method

Qblade is a multiphysics software that is widely used in the preliminary design of horizontal and vertical axis wind turbine systems on both onshore and offshore. Qblade software uses the LLFVWM method to determine the aerodynamic parameters of turbine blades (Qblade Homepage 2023). Unlike the wake approximation as in the traditional BEM method, the LLFVWM method will model explicitly the rotor wake through Lagrangian vortex elements. Therefore, the analysis results of wake effects on the rotor using LLFVWM give higher accuracy when compared with BEM (Qblade Homepage 2023; Marten *et al.* 2020; Madsen *et al.* 2020).

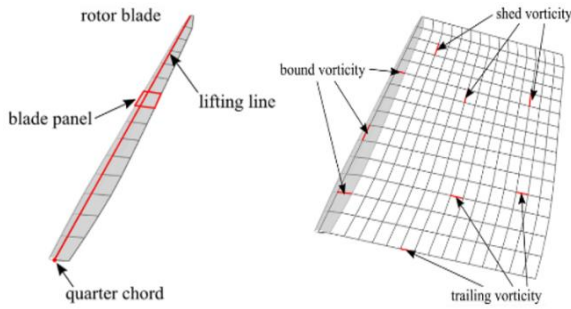


Fig 2. A blade and wake model with the LLFVWM (Qblade Homepage 2023).

In Qblade software, the blades will be divided into sections corresponding to the airfoil models and designed dimensions. Initially, the forces acting on the blades will be determined by the LLFVWM method through two dimensional sectional airfoil polar data, and the shed from the blades will be explicitly resolved. The two dimensional sectional airfoil polar data will be determined by the panel method (PM) (Drela 1989) for a specified range of angle of attack (AoA) values, and then extrapolated to the entire 360° angle. The model of a blade in Qblade software is shown in Figure 2.

Each blade will be represented by a lift line located at the chord quarter of the 2D airfoil model. The entire blade will be divided into several panels, each panel is represented by a vortex ring which consists of four straight vortex filaments as shown in Figure 2. The circulation of the bound vortex lines is calculated from the relative inflow velocity. The lift and drag coefficients were obtained from tabulated airfoil data. The sectional circulation was calculated according to the Kutta-Joukowski theorem (Bai *et al.* 2014; Valery *et al.* 2015; Eric *et al.* 2021), then the *i*th sectional lift force at the AoA is determined by the equation (1) (Qblade Homepage 2023):

$$\partial F_{Li}(AoA) = \rho V_{rel} \partial \Gamma_i \quad (1)$$

Where: $\partial F_{Li}(AoA)$ is the *i*th sectional lift force at the AoA; $\partial \Gamma_i$ is the *i*th sectional circulation; ρ is the fluid density, kg/m³; V_{rel} is the relative velocity, m/s.

Then, the aerodynamic characteristics of the entire blade such as lift force, drag force and other secondary effects will be determined in detail through several mathematical models such as OYE (Qblade Homepage 2023; Hansen *et al.* 2004) or IAG (Qblade Homepage 2023; Bangga *et al.* 2023). Previously, the model describing dynamic stall in Qblade could be implemented by using either the unsteady LLFVW or BEM via the OYE Model. However, this model only calculates the dynamics of the separated flow of airfoil. Additionally, the AoA values are only determined in the range from -50° to 50° (Qblade Homepage 2023). Recently, the IAG dynamic stall model has been developed and widely used. This model replaces the previous models in Qblade. In the study's latest (Bangga *et al.* 2023), the authors have proposed an improved IAG mathematical model and compared it with other models and experiments based on airfoil models such as S801, S809 and S814 (Ramsay *et al.* 1996; Hoffman *et al.* 1996; Ramsay *et al.* 1995; Janiszewska *et al.* 1996). This model can cover the effects of unsteady flow parameters, airfoil thickness, large changes in Reynolds number, AoA changes from -180° to 180° and also the problem of surface roughness of the airfoil models. Consequently, the aerodynamic analysis results of wind turbine

blades using Qblade software are highly accurate and reliable. Therefore, The IAG model in Qblade software was employed for this study. The IAG model in a state-space will divide the flow into three states: attached flow, separated flow and vortex lift state. Finally, the lift and drag coefficients of the blade's sections in space are determined as equations (2) and (3) (Bangga *et al.* 2023; Bangga *et al.* 2020):

$$C_{Li}^D = C_{Ni}^D \cos(AoA_i) - C_{Ti}^D \sin(AoA_i) \quad (2)$$

$$C_{Di}^D = C_{Di}^{VI} + (AoA_i - AoA_{ei}) C_{Ni}^C + (C_{Di}^{VI} - C_{D0}^{VI}) \left[\left(\frac{1 - \sqrt{x_4(t)}}{2} \right)^2 - \left(\frac{1 - \sqrt{f^{VI}}}{2} \right)^2 \right] + x_5(t) \sin \alpha_i \quad (3)$$

Where: $C_{Ni}^D = C_{Ni}^f + C_{Ni}^v$ is the normal force; $C_{Ti}^D = C_T^{VI}(AoA_{fi})$ is the tangential force; C_{Di}^{VI} , C_{D0}^{VI} , f^{VI} are the static values of drag coefficient, drag level at the zero normal force AoA and static separation position, respectively; $x_4(t)$ is the unsteady trailing edge separation point; $x_5(t)$ is the normal force due to the vortex lift effect.

2.2 The Betz optimization method

As mentioned above, in this study, the SG6043 airfoil model was used to design a complete blade. Therefore, the point coordinates of the SG6043 airfoil model (Airfoil Tools Homepage 2023) was imported into the Qblade software, the detailed configuration of the SG6043 model is shown in Figure 3. Then, the aerodynamic data of the airfoil needs to be generated using the PM method (Drela 1989), the main specific quantities such as C_l , C_d according to the different AoA values will be calculated and stored in tabular form (Qblade Homepage 2023).

In the optimization stage, the length of the entire blade and each part of the airfoil using the SG6043 model was preliminarily designed. Once the blade lengths (R) have been determined and the airfoil has been located in the blade sections (r), the chord of the airfoil (c) will be related to the TSR as equations (4) and (5) (Manwell *et al.* 2009; Magdi *et al.* 2011; Ding *et al.* 2013; Raghavendra *et al.* 2020). This is the mathematical model of BOM.

$$c(r) = \frac{8 \times \pi \times r \times \sin \varphi}{3 \times B \times C_l(r) \times TSR \times \frac{r}{R}} \quad (4)$$

$$\varphi = \tan^{-1} \left(\frac{2 \times R}{3 \times TSR \times r} \right) \quad (5)$$

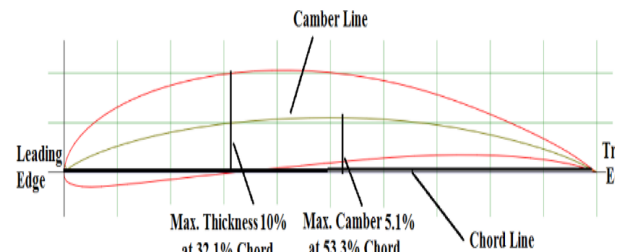


Fig 3. Layout of SG6043 airfoil.

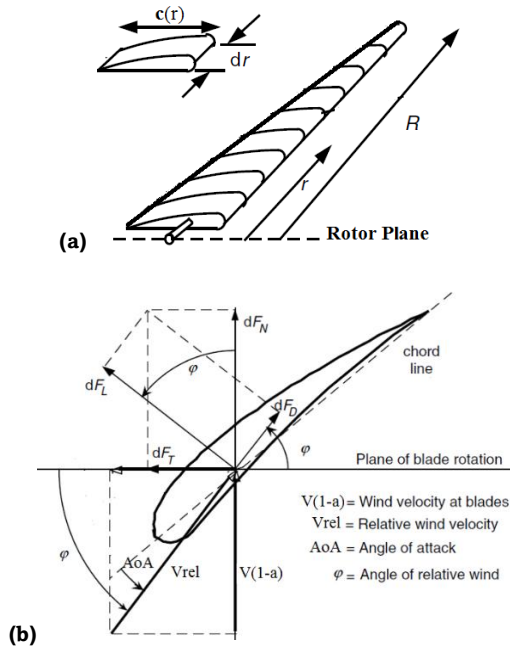


Fig 4. The blade configuration with different chord sections (a) and angles (b).

Where: $c(r)$ is the chord of the airfoil at r position, m ; B is the number of blades; $C_l(r)$ is lift coefficient of airfoil at r position. Figure 4 illustrates the blade configuration with different chord sections and angles used in the analysis.

The power factor or power coefficient is the dimensionless ratio of the extractable power to the kinetic power of the free stream. The maximum power coefficient $C_{p,max}$ is determined as the Wilson equation (Manwell *et al.* 2009):

$$C_{p,max} = \frac{16}{27} \times TSR \times \left[\frac{1.32 + \left(\frac{TSR-8}{20} \right)^2}{B^{2/3}} \right]^{-1} - \frac{0.57 \times TSR^2}{C_d \times \left(TSR + \frac{1}{2B} \right)} \quad (6)$$

With the specified number of blades, we can find the value of TSR to $C_{p,max}$ reach the maximum as shown in equation (6), then substitute this TSR value into equations (4) and equation (5) to obtain the chord values of the blade parts. This is the content of the BOM method for the shape optimization of the horizontal axis turbine blades (Xinzi *et al.* 2015; Chen *et al.* 2021).

3. Results and discussions

3.1 Reliability of the PM method

The SG6043 model was analyzed by the PM method in 2D space before being used to design the blade, the mathematical model of PM is detailed in the reports of (Drela 1989; MIT Aero. & Astro. Homepage 2023). Experimental data are referenced with the report of (Lyon *et al.* 1997), the SG6043 airfoil model will be experimentally measured with Reynolds number of 99681, corresponding to a wind speed of 4.78 m/s, and AoA values changing from -4.32° to 11.30° .

The analytical model of SG6043 airfoil using XFLR5 code in this paper was divided into $N=240$ panels and $N_{crit}=11$, the results obtained from the model are also shown in Figure 5.

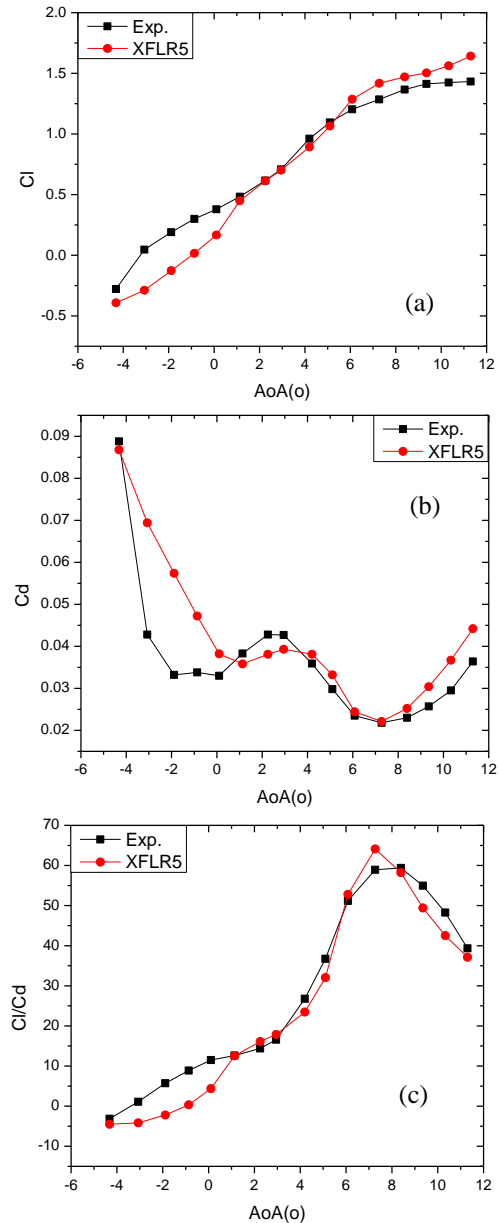


Fig 5. Compare the results obtained from experimental and analytical models.

From the results shown in Figure 5, it can be seen that the values obtained from the analytical model are very close to those obtained from the experiment. From the data, it is shown that the mean deviation between values is less than 10% and that at values around the maximum C_l/C_d position the mean error is only about 5%. This shows that the analytical model for SG6043 airfoil as in this paper has good reliability. Figure 5 shows the SG6043 airfoil according to the analytical model giving a maximum C_l/C_d value of 64.128 and at $AoA=7.27^\circ$. From here, the $AoA=7^\circ$ was selected to preliminarily determine the geometry of the airfoil in the whole blade in the following stages.

3.2 Building the blade configurations based on BOM

Turbine blades are made up of many airfoil sections at different twist angles, so in this study, the SG6043 airfoil model is also arranged at appropriate angles to create different blade configurations. Firstly, the SG6043 model was analyzed with a

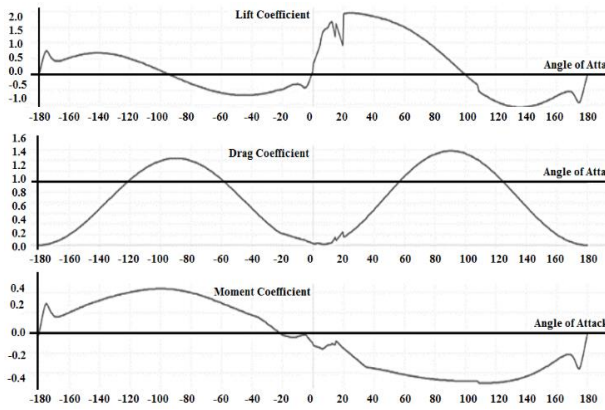


Fig 6. The 360° polar data of the SG6043 airfoil.

Reynolds number of 100000 and the AoA values changing from -10° to 20° to generate the two-dimensional sectional airfoil polar data, which is then extrapolated to the entire AoA= 360° as illustrated in Figure 6.

In the next step, the SG6043 model was put into different parts to create blades with a length of 1m to 10m using the BOM method. The relationship between quantities such as chord and twist according to the number of blades and blade length is shown in equations (4) and (5) in Section 2. There are 10 different blade configurations that were constructed and analyzed in the same manner. From the results obtained from reference papers (Shin *et al.* 2019; Mwanyika *et al.* 2021; Umar *et al.* 2022) and initial preliminary analysis, the model with TSR=7 was selected to design optimal blade configurations according to BOM. The values of chord length and twist angle

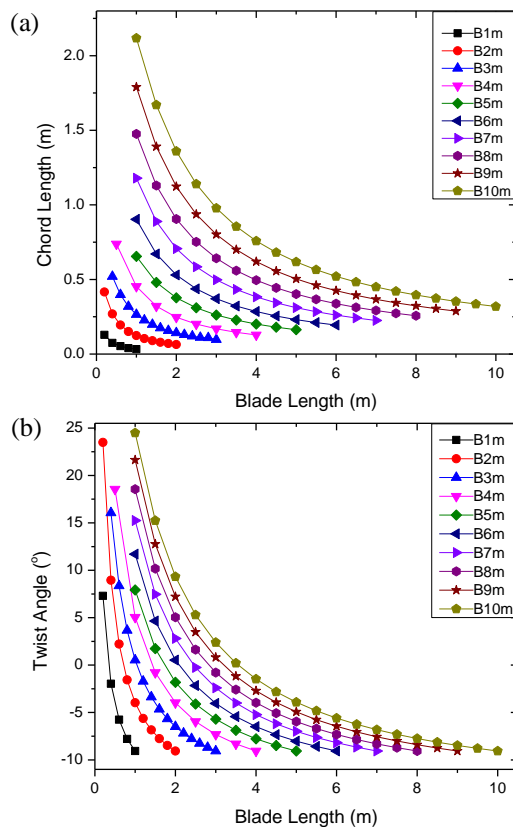


Fig 7. Distribution of chord length (a) and twist angle (b) according to the length of airfoil parts with TSR=7.

for each part of the blade are determined according to equation (4) and are shown in Figure 7.

After completing the optimal design for 10 blade configurations with different lengths, the C_p of these blades were also analyzed according to the TSR value to find the point with the highest C_p as shown in the equation (6). In the next stage, the capacity of the 3-blade rotors with different blade lengths was determined based on several mechanical settings such as pitch value, rotational speeds and wind speeds. All models in this paper use a pitch value from 1° to 15° , rotational speeds from 30rev/min to 360rev/min and wind speeds from 1m/s to 10m/s. The maximum values obtained are shown as shown in Figure 8. The maximum values are obtained when adjusting the pitch angles and rotation speeds of the rotor corresponding to each different configuration. The average pitch angle value ranges from 5° to 10° while the rotor rotation speed ranges from 30 rev/min to 330 rev/min. Rotors with longer blades have lower rotation speeds. The rotor power values in the velocity range from 1m/s to less than 3m/s are approximately zero, so they are ignored.

From Figure 8(a), it can be seen that there are huge gaps in the power coefficient value of the rotors when the blade lengths are 1m and 2m in comparison with the larger blades. The C_p value of a blade-1m rotor is only about 0.16, while for a blade-2m rotor is only about 0.25. When the rotors have a blade length of 3m or more, the C_p values change very little and gradually increase with the length. When the blade length is 10m, the maximum C_p reaches 0.476. This shows that, to effectively exploit wind energy, the rotor length must be at least 3m. Similarly, the data presented in Figure 8(b) show that the power gradually increases with the blade lengths. When the wind speed is between 3 m/s and 7m/s, the power value increases

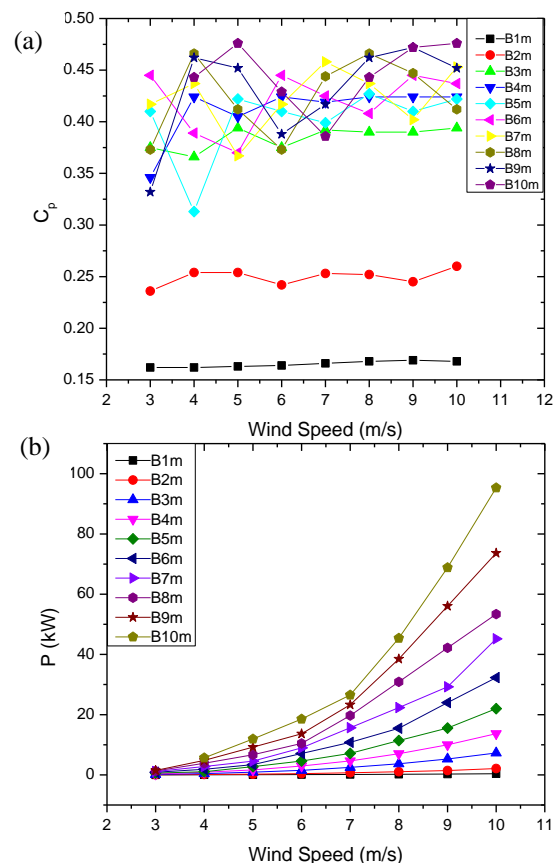


Fig 8. The maximum values of power coefficient (a) and the maximum values of power (b) according to different wind speeds.

slowly, however when the wind speed is greater than 7 m/s, the power increases dramatically and can reach 95.319 kW at a speed of 10 m/s with the 10 m long blade. The rotors with the longer blades, the more power was be obviously obtained, but the cut in wind speed will also increase gradually.

In addition, the longer blades mean that the surface area and volume of these blades also increase, which affects the fabrication, installation and operating costs. For the high velocity, such as 10 m/s, the difference in power is very large. From Figure 8(b), it is seen that rotors with blade lengths of 8m, 9m and 10m have the capacity values many times greater than the others at a wind speed of 10 m/s. Therefore, when designing a turbine for a location with such high wind speed, it is clear that the 10m blade type rotor will be the best choice. However, for the wind speed region from 4 m/s to 6 m/s, different rotors give roughly the same power. This requires to figure out which rotor configuration is best suited for this region. From there, it will take a closer look at several characteristics such as blade surface area and volume as shown in Figure 9.

The values of power at wind speed of 5 m/s in length, surface area and volume of the blades are shown in Figure 9(a),

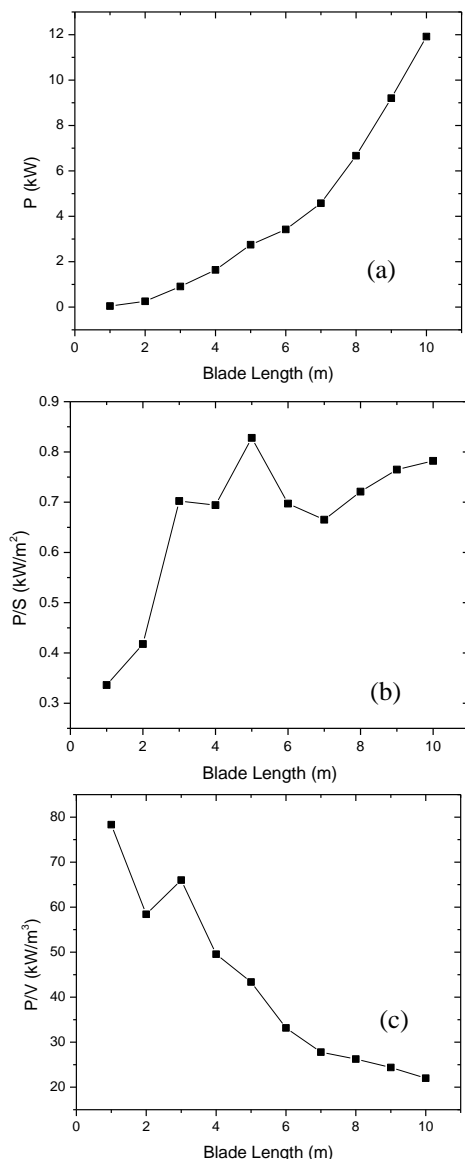


Fig 9. Power value varies with blade length (a), P/S value varies with blade length (b) and P/V value varies with blade length (c).

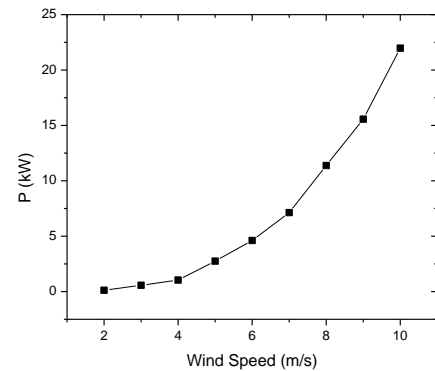


Fig 10. Power value varies with wind speed in case of 5m blade

9(b), and 9(c), respectively. From Figure 9(a), it is seen that when the blade length is from 1 m to 6 m the power increases slightly and then increased strongly until 10m. Consequently, it is determined that, if only considering the power value, the best blade length is also 10m. The capacity can reach approximately 12 kW in the case of the rotor with 10m blade.

In contrast, when considering the ratio between power and blade surface area P/S , which mainly affects the production cost of the turbine, it is found that the models have large differences in value. These values of the 1 m and 2 m blades are notably smaller compared to the rest, similar to the analysis of the power coefficient in the previous section. The remaining configurations show that the values of this ratio are considerably high, but the case with a 5m long blade is the highest as illustrated in Figure 9(b).

Regarding the volume of the blades, it is evident that the P/V of the blade lengths from 1 m to 5 m have significantly higher values than the rest of the models as shown in Figure 9(c). With the current trend in manufacturing technology, the blades of SHAWTs can be made using 3D printers. In the field of 3D printing, even minor alternations in volume and surface area of the blades can bring certain benefits in terms of both economics and manufacturing time. This directly impacts the cost of commercial products and electricity prices. However, it is important to note that while 3D printing technology offers advantages, it is still not ideal for producing large-sized products due to material limitations. From this perspective, it is determined that the blade models with lengths of 1m to 5m are suitable for fabrication and individual household use. However, rotors using the 1m long blades and the 2 m long blades with only 0.047 kW and 0.257 kW at a wind speed of 5 m/s will not meet the electricity consumption of each household.

According to statistical reports on electricity consumption in recent years, electricity consumption per capita in Vietnam is about 2000kWh per year (Institute of Energy 2023; WorldData 2023; EnerData 2023; IEA 2023; Juliet *et al.* 2023). Typically, each family consists of about 3 to 5 people, requiring approximately about 16 kWh to 27 kWh of electricity per day. Thus, the average household in Vietnam requires approximately 20kWh of electricity per day. Assuming an average duration of wind at a speed of 5 m/s per day is 8 hours, it is necessary to use a rotor configuration with 5m long blades. Therefore, the rotor model using the 5 m long blades with a capacity of 2.750 kW at a rated wind speed of 5 m/s is proposed as the most beneficial and suitable SHAWT model for each household to use. The capacity of the 5m blade configuration varies with wind speed as shown in Figure 10.

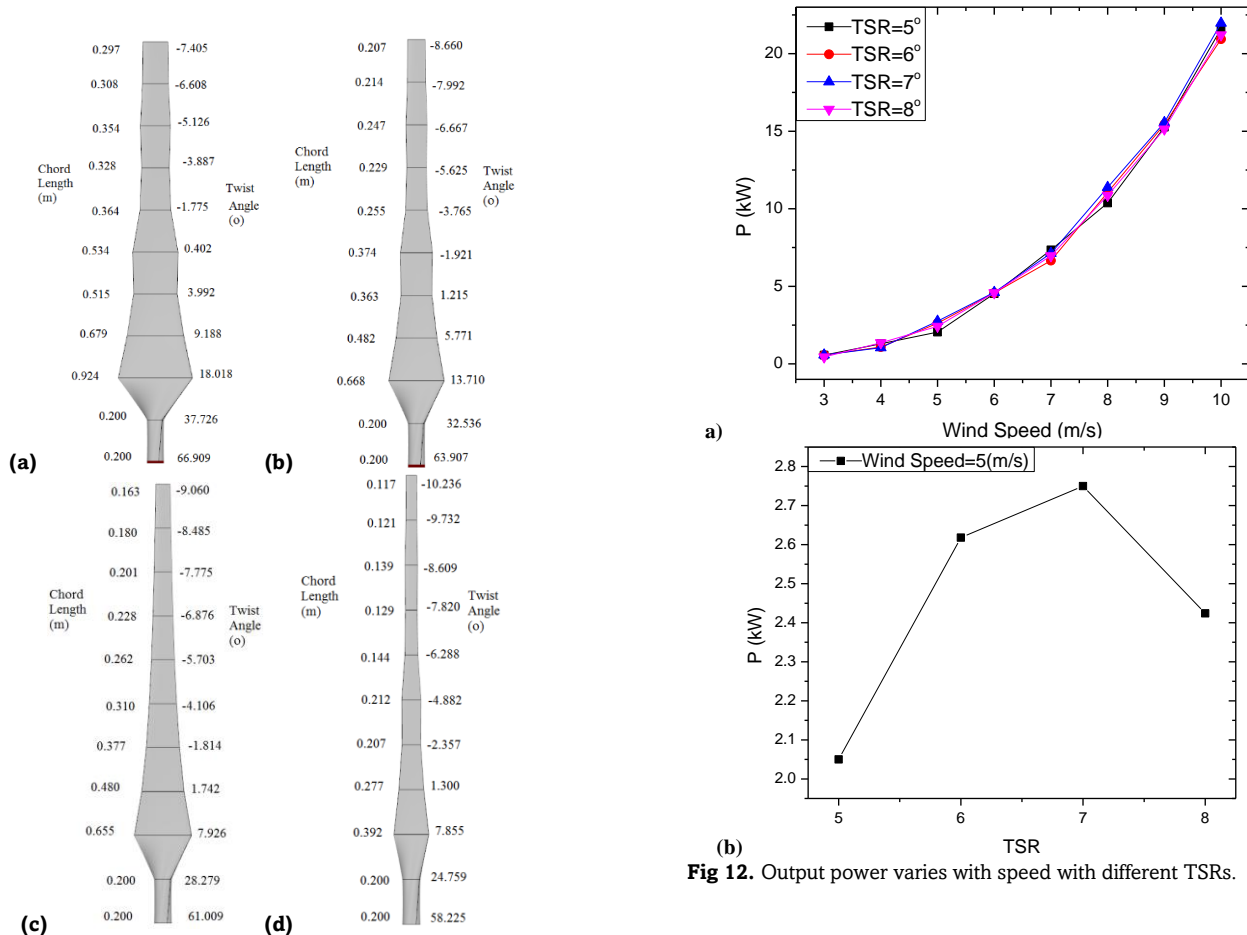


Fig 11. Detailed configurations of the 5m blade model with STR=5 (a), TSR=6 (b), TSR=7 (c) and TSR=8 (d)

Based on the obtained results after analysing ten different configurations of the turbine, the blade model with length of 5m was proposed to choose as the most suitable for practical usage in Vietnam. However, to make sure that the 5 m blade model with TSR=7 is optimal, it is continued to design additional 5m blade models with TSRs of 5, 6 and 8 respectively. Then, all 4 models were analysed and compared both in terms of appearance and output power under similar operating conditions. Detailed layouts of four different types are shown in Figure 11 and the power values are shown in Figure 12. From Figure 10, it is observed that the width of the 5m blade pattern is larger for the case of smaller TSR. This implies that with a small TSR, the blade surface area will be larger, resulting in higher raw material consumption and production costs. Moreover, larger blades will entail heavier mass, leading to larger support tower systems and consuming more materials and land area.

From Figure 11, it is realized that the capacity gradually rises while the TSR increases from 5 to 7. When TSR= 8, the capacity value begins to decrease. Considering the case of operation at a wind speed of 5 m/s, the difference between these types can be up to about 13.41%. Thus, it is firmly confirmed that blade models using TSR=7 offer the most optimal configuration. The main reason for the difference in power factor and power being larger as the width of the blade (Reynolds number) is higher is the wake effect. When wind strikes the front surface of the rotor blades, the friction between the wind layer in direct contact with the blade surface will create vortices and separation at the blade surface. This separation

appears from the front part of the air-foil and gradually shifts back as the wind speed increases. The consequence of this effect will be to reduce the lift coefficient and increase the drag coefficient of each air-foil part and the entire blade. In these four models, the chord length of the blade models increases as the TSR gets decreases, leading to an increase in the Reynolds number. Therefore, the effects of the wake will tend to increase as the chord length increases. On the contrary, when the chord length is too small, it will lead to a smaller Reynolds number below the turbulent flow level, moving into the transition flow region. This in turn causes the wake effect to fluctuate, making it difficult to determine and resulting in a decrease in the ration between the lift coefficient and drag coefficient (Martin *et al.* 2023; Václav *et al.* 2019).

A summary of some turbine blade designs based on the SG6043 model obtained from other research groups is shown in Table 1. It can realize certain limitations, which render the turbines impractical and ineffective in wind energy exploitation. For example, the turbine in reference (Umar *et al.* 2022) only achieves a capacity of 80.1 W, equivalent to the power consumption of a light bulb, making it insufficient to meet the minimum electricity demand of a household. Additionally, the turbine designs presented in references (Akbari *et al.* 2022; Daniyan *et al.* 2018) operate at excessively high wind speeds. If there are areas with such high wind speeds, the turbines with blades up to hundreds of meters long should be used. Furthermore, the designs proposed in the references (Mwanyika *et al.* 2021; Mostafa *et al.* 2014) offers reasonable power values. Data from Figure 10 shows that the turbine model with 5m long blades has a capacity equivalent to the model of Mostafa *et al.* (2014) at a speed of 6m/s. However, with a wind speed of 8 m/s, the turbine model introduced in the study has a

Table 1
Compare results obtained from several types of rotors by other research groups

References	Blade Length (m)	Rated Wind Speed (m/s)	Power (W)
Umar <i>et al.</i> (2022)	1.00	4	80.1
Akbari <i>et al.</i> (2022)	1.21	10	1000.0
Daniyan <i>et al.</i> (2018)	0.50	18	1108.0
Mwanyika <i>et al.</i> (2021)	3.56	8	5258.0
Mostafa <i>et al.</i> (2014)	4.46	6	5128.0
This study	5.00	5	2750.0

capacity of 11,379 kW, a value much larger than the turbine model introduced by Mwanyika *et al.* (2021). This clearly demonstrates the superiority of this new turbine model compared to previously announced models. However, the turbine models with 5m blades need to be built within a wide enough range to ensure safety during operation. Therefore, these types of turbines should only be used in rural and mountainous areas where there are large land areas. Finally, the new design proposed in this study is more practical and can bring more benefits to people who can proactively supply electricity to their families.

4. Conclusion

The article has presented the optimal design method for wind turbine blades based on the SG6043 model operating in the wind speed range between 1 m/s and 10 m/s, thereby providing blade configurations with different lengths from 1m to 10m. The analysis process shows the BOM method is the optimal design method for fast results, reducing costs and calculation time. In addition, the PM method for preliminary aerodynamic calculations of the airfoil model, combined with the newly updated models in Qblade gives results with acceptable accuracy for the entire wind turbine rotor. Turbine blade designs are considered based on power, blade surface area and blade volume values. The main advantage is that these designs can be produced by using the promising 3D printing technology. It helps to select blades that provide greater capacity with smaller volume and surface area. Therefore, this has practical applications and bring many economic benefits.

The SG6043 airfoil model demonstrates high aerodynamic efficiency and is suitable for designing the blades of SHAWTs in conditions with wind speeds of less than 10 m/s. The wind energy exploitation efficiency of a turbine using the SG6043 blade model can reach 47.6%, a value much higher than small capacity turbines and equivalent to large commercial turbines. Turbines operate with higher efficiency, which means increased economic benefits and contributes to more sustainable development. For wind areas with a speed of 5 m/s, blades with a length of 3 m to 5 m offer better production, installation and operation efficiency than other configurations. However, if considering the electricity demand, the rotor using 5m long blades will be most suitable for individual households in Vietnam. This will consequently reduce the generated electricity from coal-fired power plants and thus contribute to relieving environmental pollution and climate change. This is one of the energy solutions for Vietnam to achieve its net-zero emissions target by 2050.

Author Contributions: D. V. T.: Conceptualization, methodology, formal analysis, writing—original draft; N. H. D.: supervision, resources, project administration, writing—review and editing, validation; L. Q. S.: supervision, resources, project administration, writing—review and editing, validation. All authors have read and agreed to the published version of the manuscript.

Conflicts of Interest: The authors declare no conflict of interest.

References

Akbari, V., Naghashzadegan, M., Kouhikamali, R., Afsharpanah, F., Yaici, W. (2022). Multi-objective optimization and optimal airfoil blade selection for a small horizontal-axis wind turbine for application in regions with various wind potential. *Machines*, 10 (8), 1-22. <https://doi.org/10.3390/machines10080687>.

Anupam, K., Abdulkareem, Sh., Mahdi, A. O., Lee, C. H. (2023). A comprehensive review of innovative wind turbine airfoil and blade designs: Toward enhanced efficiency and sustainability. *Sustainable Energy Technologies and Assessments*, 60, 103511. <https://doi.org/10.1016/j.seta.2023.103511>.

Airfoil Tools Homepage (2023) *Airfoil SG6043*. <http://airfoiltools.com/airfoil/details?airfoil=sg6043-il>. Accessed on 12 December 2023.

Bangga, G., Lutz, T., Arnold, M. (2020). An improved second-order dynamic stall model for wind turbine airfoils. *Wind Energy Sci.*, 5, 1037–1058. <https://doi.org/10.5194/wes-5-1037-2020>.

Bangga, G., Parkinson, S., Collier, W. (2023). Development and validation of the iag dynamic stall model in state-space representation for wind turbine airfoils. *Energies*, 16 (10), 1-25. <https://doi.org/10.3390/en16103994>.

Bai, C. and Wu, Z. (2014). Generalized Kutta–Joukowski theorem for multi-vortex and multi-airfoil flow (a lumped vortex model). *Chinese Journal of Aeronautics*, 27 (1), 34–39. <https://doi.org/10.1016/j.cja.2013.07.022>.

Chen, Y., Hu, D. and Zhao, Z. (2021). Low-speed wind turbine design based on Wilson theory. *IOP Conf. Series: Earth and Environmental Science*, 621 (2021) 012175. <https://doi.org/10.1088/1755-1315/621/1/012175>

Daniyan, I. A., Daniyan, O. L., Adeodu, A. O., Azeez, T. M., Ibekwe, K. S. (2018). Design and Simulation of a Wind Turbine for Electricity Generation. *International Journal of Applied Engineering Research*, 13(23), 16409-16417. https://www.ripublication.com/ijaer18/ijaerv13n23_33.pdf

Ding, J. J., Wang, H., Sun, L. P. and Ma, B. (2013). Optimal Design of Wind Turbine Blades with Wilson and BEM Method Integrated. *In Applied Mechanics and Materials*, 404, 286–291. <https://doi.org/10.4028/www.scientific.net/amm.404.286>.

Drela, M. (1989) *XFOIL: An Analysis and Design System For Low Reynolds Number Airfoils*. MIT Dept. of Aeronautics and Astronautics, Cambridge, Massachusetts.

EnerData (2023) *Vietnam Energy Information*. <https://www.enerdata.net/estore/energy-market/vietnam/>. Accessed on 12 December 2023.

EIA (2023) *Wind explained: Types of wind turbines*. <https://www.eia.gov/energyexplained/wind/types-of-wind-turbines.php>. Accessed on 12 December 2023.

Eric J. L. and David H. W. (2021). An impulse-based derivation of the Kutta–Joukowski equation for wind turbine thrust. *Wind Energ. Sci.*, 6, 191–201, 2021. <https://doi.org/10.5194/wes-6-191-2021>.

Giguere, P., Selig, M. S. (1998). New airfoils for small horizontal axis wind turbines. *Journal of Solar Energy Engineering*, 120, 108-114. <https://doi.org/10.1115/1.2888052>

Hansen, M. H., Gaunaa, M., Madsen, H. A. (2004) *A Beddoes-Leishman type dynamic stall model in state-space and indicial formulation*. Technical Report, DTU.

Hoffman, M., Ramsay, R., Gregorek, G. (1996) *Effects of Grit Roughness and Pitch Oscillations on the NACA 4415 Airfoil*. Technical Report. National Renewable Energy Lab.: Golden, CO, USA.

IEA (2023) *Vietnam*. <https://www.iea.org/countries/vietnam>. Accessed on 12 December 2023.

- Institute of Energy (2023) *The national power development plan in the 2021-2030 period, with vision to 2050*. Ministry of Industry and Trade of The Socialist Republic of Vietnam, (in Vietnamese).
- IRENA (2022) *World energy transitions outlook 2022: 1.5°C pathway*. International Renewable Energy Agency, Abu Dhabi. <https://www.irena.org/Digital-Report/World-Energy-Transitions-Outlook-2022>
- James M., Jon M., Anthony R. (2009) *Wind energy explained: theory, design, and application – 2nd ed.* John Wiley & Sons Ltd.. <https://doi.org/10.1260/030952406778055054>
- Janiszewska, J., Ramsay, R., Hoffman, M., Gregorek, G. (1996) *Effects of Grit Roughness and Pitch Oscillations on the S814 Airfoil*. Technical Report. National Renewable Energy Lab.: Golden, CO, USA. <https://www.osti.gov/biblio/273772>
- Juliet D. and Nick W. (2023) *The 72nd Statistical Review of World Energy*. ISBN: 9781787253797. Energy Institute (EI). https://www.energyinst.org/_data/assets/pdf_file/0004/1055542/EI_Stat_Review_PDF_single_3.pdf
- Karthikeyan, N., Kalidasa, M. K., ArunKumar, S., Rajakumar, S. (2015). Review of aerodynamic developments on small horizontal axis wind turbine blade. *Renewable and Sustainable Energy Reviews*, 42, 801–822. <https://doi.org/10.1016/j.rser.2014.10.086>.
- Lyon, C. A., Broeren, A. P., Giguere, P., Gopalathnam, A., Selig, M. S. (1997) *Summary of low-speed airfoil data-volume 3*. SoarTech Publications. Virginia Beach. https://m-selig.ae.illinois.edu/uiuc_lsar/Low-Speed-Airfoil-Data-V3.pdf
- Madsen, H. A., Larsen, T. J., Pirrung, G. R., Li A., Zahle F. (2020). Implementation of the blade element momentum model on a polar grid and its aeroelastic load impact. *Wind Energy Science*, volume 5 (1): 1–27. <https://wes.copernicus.org/articles/5/1/2020/>, doi:10.5194/wes-5-1-2020.
- Magdi, R. and Adam, M. R. (2011) *Wind Turbines Theory - The Betz Equation and Optimal Rotor Tip Speed Ratio*, Fundamental and Advanced Topics in Wind Power. ISBN: 978-953-307-508-2. InTech. https://cdn.intechopen.com/pdfs/16242/InTech-Wind_turbines_theory_the_betz_equation_and_optimal_rotor_tip_speed_ratio.pdf
- Marten, D., Paschereit, C. O., Huang, X., Meinke, M., Schröder, W., Müller, J., Ober-leithner, K. (2020). Predicting wind turbine wake breakdown using a free vortex wake code. *AIAA Journal*, 58 (11), 4672–4685. <https://doi.org/10.2514/6.2019-2080>.
- Martin B., Michaël P., Florent R. (2023). Experimental investigation of the effects of the Reynolds number on the performance and near wake of a wind turbine. *Renewable Energy*, 209, 63-70. <https://10.1016/j.renene.2023.03.093>.
- MIT Aero. & Astro. Homepage (2023) *Xfoil Documentation*. https://web.mit.edu/drela/Public/web/xfoil/xfoil_doc.txt. Accessed on 12 December 2023.
- Mostafa, N. H., Talaat, M., Ibrahim, M. M. (2014). Performance analysis and design a small horizontal axis wind turbine. *41st Annual Conference, The Association of Egyptian - American Scholars*, pp. 1-8. https://www.researchgate.net/publication/332514429_Performance_Analysis_and_Design_a_Small_Horizontal_Axis_Wind_Turbine
- Mwanyika, H. H., Jande, Y. A., Kivevele, T. (2021). Design and performance analysis of composite airfoil wind turbine blade. *Tanzania Journal of Science*, 47 (5), 1701-1715. <https://dx.doi.org/10.4314/tjs.v47i5.18>
- Qblade Homepage (2023) *Qblade Documentation*. <https://docs.qblade.org/>. Accessed on 12 December 2023.
- Raghavendra, S., Ravikumar, T., Gnaendra, R., Manjunatha, K. and Madhusudhana, S. (2020). Design of wind blades for the development of low-power wind turbines using Betz and Schmitz methods. *Advances in Materials and Processing Technologies*, 8 (1), 808-827. <https://doi.org/10.1080/2374068X.2020.1833605>.
- Ramsay, R., Hoffman, M., Gregorek, G. (1995) *Effects of Grit Roughness and Pitch Oscillations on the S809 Airfoil*. Technical report. National Renewable Energy Lab.: Golden, CO, USA. <https://www.osti.gov/biblio/205563>
- Ramsay, R., Hoffman, M., Gregorek, G. (1996) *Effects of Grit Roughness and Pitch Oscillations on the S801 Airfoil*. Technical Report. National Renewable Energy Lab.: Golden, CO, USA. <https://www.osti.gov/biblio/204225>
- Shin, P., Kim, K. (2019). Aerodynamic performance prediction of SG6043 airfoil for a horizontal-axis small wind turbine. *Journal of Physics: Conference Series* 1452, NAWEA WindTech, pp. 1-11. <https://doi.org/10.1088/1742-6596/1452/1/012018>.
- Suhas, B.G., Sreejith, B.K., Chandra, A.R.A. (2023). Design of a low velocity wind turbine blades for power generation: part I-aerodynamic performance. *Sādhanā*, volume 48, 276. <https://doi.org/10.1007/s12046-023-02339-1>.
- Umar, D. A., Yaw, C. T., Koh, S. P., Tiong, S. K., Alkahtani, A. A., Yusaf, T. (2022). Design and optimization of a small-scale horizontal axis wind turbine blade for energy harvesting at low wind profile areas. *Energies*, volume 15 (9), 1-22. <https://doi.org/10.3390/en15093033>.
- Valery L. O., Jens N. S., David H. W. (2015). The rotor theories by Professor Joukowsky: Vortex theories. *Progress in Aerospace Sciences*, volume 73, February 2015, 19-46. <https://doi.org/10.1016/j.paerosci.2014.10.002>.
- Václav, U., Pavel, P. (2019). The Reynolds number effect on dynamics of the wake behind a circular cylinder. *AIP Conf. Proc.* 2189, 020023. <https://doi.org/10.1063/1.5138635>.
- Wind Energy Technologies Office (2023) *Land-Based Wind Market Report: 2023 Edition*. <https://www.energy.gov/eere/wind/articles/land-based-wind-market-report-2023-edition>. Accessed on 12 December 2023.
- WindExchange (2023) *Small Wind Guidebook*. <https://windexchange.energy.gov/small-wind-guidebook>. Accessed on 12 December 2023.
- WorldData (2023) *Vietnam Energy Consumption*. <https://www.worlddata.info/asia/vietnam/energy-consumption.php>. Accessed on 12 December 2023.
- Xinzi, T., Xuanqing, H., Ruitao, P., Xiongwei, L. (2015). A Direct Approach of Design Optimization for Small Horizontal Axis Wind Turbine Blades. *Procedia CIRP*, 36, 12–16. <https://doi.org/10.1016/j.procir.2015.01.047>.

